MI-TH-1601

Diphoton Excess in Consistent Supersymmetric $SU(5)$ Models with Vector-like Particles

Bhaskar Dutta,[1] Yu Gao,[1] Tathagata Ghosh,[1] Ilia Gogoladze,[2]
Tianjun Li,[3,4] Qaisar Shafi,[2] and Joel W. Walker[5]

[1]*Mitchell Institute for Fundamental Physics and Astronomy,*
Department of Physics and Astronomy,
Texas A&M University, College Station, TX 77843-4242, USA

[2]*Bartol Research Institute, Department of Physics and Astronomy,*
University of Delaware, Newark, DE 19716, USA

[3]*State Key Laboratory of Theoretical Physics and Kavli Institute for*
Theoretical Physics China (KITPC), Institute of Theoretical Physics,
Chinese Academy of Sciences, Beijing 100190, P. R. China

[4]*School of Physical Electronics, University of Electronic Science*
and Technology of China, Chengdu 610054, P. R. China

[5]*Department of Physics, Sam Houston State University, Huntsville, TX 77341, USA*

(Dated: January 6, 2016)

Abstract

We consider the diphoton resonance at the 13 TeV LHC in the context of $SU(5)$ grand unification. A leading candidate to explain this resonance is a standard model singlet scalar decaying to a pair of photon by means of vector-like fermionic loops. We demonstrate the effect of the vector-like multiplets $(5, \overline{5})$ and $(10, \overline{10})$ on the evolution of the gauge couplings and perturbatively evaluate the weak scale values of the new couplings and masses run down from the unification scale. We use these masses and couplings to explain the diphoton resonance after considering the new dijet constraints. We show how to accommodate the larger decay width of the resonance particle, which seems to be preferred by the experimental data. In addition, we consider new couplings relating various components of $(5, \overline{5})$ and $(10, \overline{10})$ in the context of the orbifold GUTs, where the resonance scalar can be a part of the new vector-like lepton doublets. We also calculate the Higgs mass and proton decay rate $p \to e^+\pi^0$ in the context of $SU(5)$ grand unification, including effects of the new vector-like multiplets.

PACS numbers: 11.10.Kk, 11.25.Mj, 11.25.-w, 12.60.Jv

I. INTRODUCTION

Supersymmetry (SUSY) provides an elegant solution to the gauge hierarchy problem in the Standard Model (SM). In addition it has many appealing features. In Supersymmetric SMs (SSMs) with R-parity, we can realize gauge coupling unification, have the Lightest Supersymmetric Particle (LSP), namely the neutralino, as a dark matter candidate, radiatively break the electroweak gauge symmetry, etc. In particular, gauge coupling unification strongly supports the Grand Unified Theories (GUTs), and supersymmetry is thus a bridge between the low energy phenomenology and high-energy fundamental physics.

It is well known that a SM-like Higgs boson with mass m_H around 125 GeV was discovered during the first run of the LHC [1, 2]. In the Minimal SSM (MSSM), to realize such a Higgs boson mass it is necessary to have either multi-TeV top squarks with small mixing or TeV-scale top squarks with large mixing, which might increase the fine-tuning or induce $SU(3) \times U(1)_{\rm EM}$ gauge symmetry breaking, respectively. On the other hand, it has long been understood that one can extend the matter sector of the MSSM and still preserve the elegant result of gauge coupling unification if the new matter fields form complete multiplets of $SU(5)$. To automatically cancel the gauge anomalies, we assume here that such supermultiplets are vector-like. In fact, complete light GUT multiplets of this variety are not unexpected. Within string theory one often finds light multiplets in the spectrum [3], and even within the GUT framework itself one can encounter extra complete multiplets lying at the TeV scale [4]. Similarly to the top quark contribution, the Higgs boson mass can be lifted by the Yukawa couplings between these vector-like particles and the Higgs fields. Consequently, the SM gauge couplings will become stronger at the GUT scale, in which case the proton lifetime will be reduced, thus coming within the reach of proton decay experiments such as Hyper-Kamiokande.

Recently, both the ATLAS [5] and CMS [6] collaborations have reported an excess of events in the diphoton channel with invariant mass of about 750 GeV at the 13 TeV LHC. With an integrated luminosity of 3.2 fb^{-1}, the ATLAS collaboration has observed a local 3.6σ excess at a diphoton invariant mass of around 747 GeV, assuming a narrow width resonance. For a wider width resonance, the signal significance increases to 3.9σ with a preferred width of about 45 GeV. With an integrated luminosity of 2.6 fb^{-1}, the CMS collaboration has also observed a diphoton excess with a local significance of 2.6σ at invariant mass of around 760 GeV. Assuming a decay width of around 45 GeV, the significance reduces to 2σ in this case. The corresponding excesses in the cross section can be roughly estimated as $\sigma^{13~\rm TeV}_{pp\to\gamma\gamma} \sim 3 - 13$ fb [5, 6]. Interestingly, the CMS collaboration did likewise search for diphoton resonances [7] at $\sqrt{s} = 8$ TeV and observed a slight excess $\sim 2\sigma$ at an invariant mass of about 750 GeV, but the ATLAS collaboration did not go beyond the mass of 600

GeV for this channel [8]. Thus, the present ATLAS and CMS results the $\sqrt{s} = 13$ TeV are indeed consistent with those at the $\sqrt{s} = 8$ TeV LHC in the diphoton channel. The dijet constraints from LHC may strongly constrain any interpretation of this resonance. The CMS collaboration has recently reported a new analysis on dijet final state resonances [9]. We investigated the compatibility of our explanation of the resonance against this result.

A straightforward approach to explaining the diphoton excess is the introduction of a SM singlet S with mass of 750 GeV and accompanying multiplets of vector-like particles. With vector-like particles in the loops, the singlet S can be produced via gluon fusion, and can likewise decay into a diphoton pair. The diphoton excess, in a non-supersymmetric context, was previously addressed by some of the authors using vector-like particles, as motivated by solutions to the gauge unification, neutrino mass, and electroweak vacuum stability problems [10]. This approach can be naturally embedded in the SSMs with vector-like particles. In this paper, we study gauge coupling unification, calculate the Higgs boson mass, and estimate the diphoton event rate. After careful study, we find that one needs to be careful about how may copies of multiplets and corresponding couplings are required to explain the diphoton resonance while still achieving the gauge coupling unification. A recent analysis [11] of CMS and ATLAS data and a fit to the combined run-I and run-II data indicates that the resonance at 750 GeV can be accommodated by $\sigma_{\gamma\gamma} \sim 0.7 - 16$ fb for $\Gamma_S \sim 5 - 100$ GeV at 2σ level. We explore the capacity of $(10, \overline{10})$ and $(5, \overline{5})$ multiplets to explain the resonance. We additionally demonstrate how to accommodate a larger resonance width in the context of this unified scenario by introducing decays of the scalar to soft leptons with very little missing energy, which is allowed by current experimental data. We point out that the proton lifetime estimates lie within reach of the future Hyper-Kamiokande experiment.

We also show that the neutral component of the vector-like lepton doublets can be utilized to explain the excess. In this case these doublets are R-parity even, which moreover will not induce proton decay problems. Such scenarios can be realized in the orbifold GUTs [12–14] and F-theory GUTs [15–18] (see Ref. [19] and references therein). The requirement of two new doublets in this scenario allows for the possibility of two adjacent resonances, which can be useful to generate the appearance of a large effective width.

This excess, although still statistically not significant, has drawn immense attention from from the particle physics community resulting in diverse explanations ranging from axions, extended Higgs sectors to dark matter [10, 11, 20–25]. In two recent papers [22, 23], the diphoton excess has been addressed in the context of $SU(5)$ grand unification. In our paper, however, we have included the new dijet constraint in order to estimate the number of vector-like multiplets necessary to address the diphoton excess, which we then utilize to calculate the Higgs mass. We additionally consider a new interaction involving the neutral scalar from vector-like doublets to explain the excess. We also show new ways to handle the larger resonance width and associated final states.

The paper is organized as follows. In section II, we discuss the GUT models with vector-like particles and projections for proton decay. In section III, we discuss the impact on Higgs Boson mass arising from vector-like particles. In section IV, we discuss the neutral component of vector-like doublets as a resonance candidate, and in section V, we discuss the diphoton resonance. We conclude in section VI.

II. GUT MODELS WITH VECTOR-LIKE PARTICLES AND PROTON DECAY

It is well known that matter fields will contribute at one loop to the CP-even Higgs mass if there are direct couplings between them and the Higgs fields. We will elaborate upon these additional contributions in the next section. On the other hand, there are constraints on the couplings and masses of new matter fields if they are involved in chiral symmetry breaking interactions. The most important constraints are the S and T parameters, which limit the number of extra *chiral* generations. Consistent with these constraints, one should add new matter fields which are predominantly vector-like.

In the limit where the vector-like mass is much heavier than the chiral mass terms arising from Yukawa couplings to the Higgs doublets, the contribution to the T parameter from a single chiral fermion is approximately [26]:

$$\delta T = \frac{N(\kappa v)^2}{10\pi \sin^2\theta_W m_W^2}\left[\left(\frac{\kappa v}{M_V}\right)^2 + O\left(\frac{\kappa v}{M_V}\right)^4\right], \tag{1}$$

where κ is the new chiral Yukawa coupling, v is the Vacuum Expectation Value (VEV) of the corresponding Higgs field, and N counts the additional number of $SU(2)$ doublets. For instance, $N = 3$ if $(10, \overline{10})$ is considered at low scale, while $N = 1$ for the $(5, \overline{5})$ case. It is known that from precision electroweak data $T \leq 0.2$ at 95% CL for $m_h = 125$ GeV [27]. We will take $\delta T < 0.2$ as a realistic bound in our analysis. We then see from Eq. (1) that with M_V around 1 TeV, the Yukawa coupling κ can be $O(1)$.

A strong constraint on the nature of new vector-like particle arises from the perturbativity and unification conditions. One finds that the following combinations of low-energy (TeV-scale) vector-like particles may be introduced safely: *(i)* up to 4 pairs of $(5, \overline{5})$'s, or *(ii)* one pair of $(10, \overline{10})$, or *(iii)* one pair each of $(5, \overline{5})$ and $(10, \overline{10})$. The last option also neatly fits into the $(16 + \overline{16})$ representation of $SO(10)$ if an additional pair of singlets are added. We will thus refer to case *(iii)* as $(16 + \overline{16})$.

We illustrate in Figure 1 how gauge coupling running is modified by introducing different sets of vector-like particles. In particular, examples of the gauge coupling evolution are

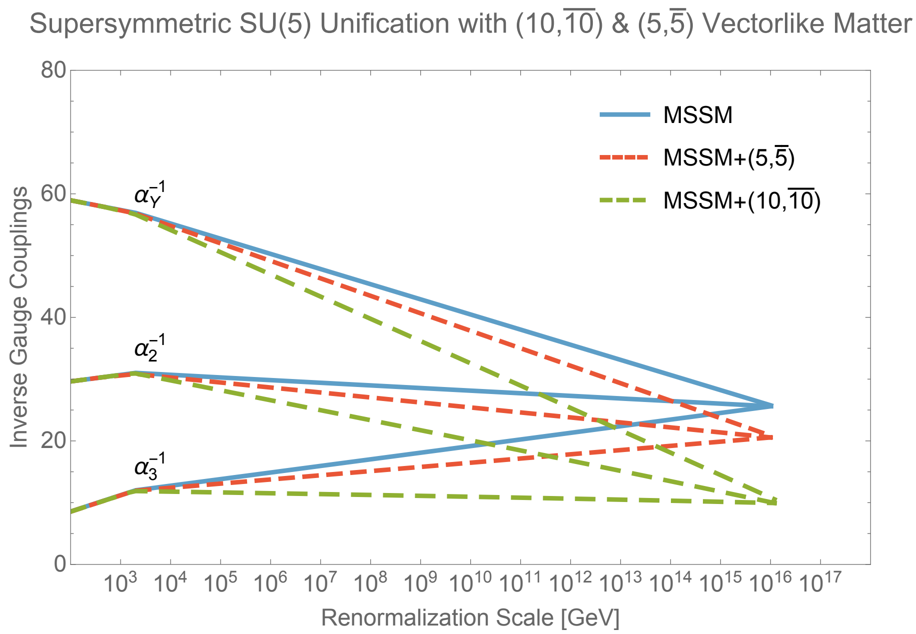

FIG. 1. Gauge coupling evolution with the effective SUSY breaking scale $M_S = 2$ TeV and $\tan\beta = 10$. Solid lines correspond to the MSSM. Short dashed lines correspond to the MSSM+$(5, \bar{5})$. Long dashed lines are for MSSM plus $(10, \overline{10})$, which is essentially the same as MSSM plus $3 \times (5, \bar{5})$. Vector-like masses are set at $M_V^Q = 1$ TeV and $M_V^L = 400$ GeV.

plotted for the case of MSSM by itself and MSSM plus the complete $SU(5)$ multiplets $(10 + \overline{10})$ and $(5 + \bar{5})$. The GUT-scale $M_{\rm GUT}$ and unified coupling $\alpha_{\rm GUT}$ applicable to each of the itemized scenarios are further presented numerically in Table I. RGEs are run at two loops in the gauge sector, with feedback from the one loop MSSM Yukawa couplings. For uniformity, all entries in Table I, as well as Figure 1, are computed for colored and non-colored vector-like masses of $M_V^Q = 1$ TeV and $M_V^L = 400$ GeV, with all sparticles (including the scalar vector-like partners) at $M_{\rm SUSY} = 2$ TeV, and $\tan\beta = 10$. The residual gap $\Delta_{Y2} \equiv |g_Y - g_2| \div (g_Y + g_2)$ between the hypercharge and $SU(2)_{\rm L}$ couplings at the scale where the perturbative unification $\alpha_3 = \alpha_2$ occurs is less well controlled in the $(16 + \overline{16})$ scenario, but this may be mitigated substantially by elevating the SUSY scale into the several TeV range.

We next consider the rate of proton decay $p \to e^+\pi^0$ via dimension-6 operators from heavy gauge boson exchange, in keeping with the prescription of Ref. [33].

$$\tau_p(e^+\pi^0) \simeq 1.0 \times 10^{34} \times \left(\frac{2.5}{A_R}\right)^2 \times \left(\frac{0.04}{\alpha_{\rm GUT}}\right)^2 \times \left(\frac{M_{\rm GUT}}{1.0 \times 10^{16}\ {\rm GeV}}\right)^4 \ \text{years} \tag{2}$$

The lifetime scales as a fourth power of the unification scale $M_{\rm GUT}$, as an inverse-squared power of the unified coupling $\alpha_{\rm GUT}$, as an inverse-squared power of the hadronic matrix element $\alpha_{\rm H}$ [34], and as an inverse-squared power of the dimensionless 1-loop renormalization

$N(10,\overline{10})$	$N(5,\overline{5})$	M_{GUT}	α_{GUT}	Δ_{Y2}	A_R^{SD}	$\tau_{\text{p}}(e^+\pi^0)$
0	0	1.1	0.039	0.001	2.0	14
0	1	1.1	0.049	0.003	2.4	6.9
0	2	1.2	0.065	0.004	3.1	3.2
0	3	1.4	0.10	0.007	4.3	1.5
0	4	2.7	0.30	0.007	6.7	0.93
1	0	1.2	0.10	0.016	4.3	0.76
1	1	1.6	0.30	0.070	6.8	0.10

TABLE I. Unification parameters and proton lifetime projections for various configurations of $SU(5)$ vector-like supermultiplets taken in addition to the field content of the MSSM. The scale M_{GUT} at which $\alpha_3 = \alpha_2 = \alpha_{\text{GUT}}$ is given in units of 10^{16} [GeV]. The ratio Δ_{Y2} represents the fractional separation of α_Y and α_2 at the GUT scale. The dimensionless factors A_R^{SD} reflect short-distance renormalization of the anomalous dimension associated with relevant baryon-number violating operators. The proton lifetime τ_{p} in the dimension-six $e^+\pi^0$ channel is projected in units of 10^{34} [y]. All entries are computed for vector-like masses $M_V^Q = 1$ TeV and $M_V^L = 400$ GeV, with all sparticles at $M_{\text{SUSY}} = 2$ TeV, and $\tan\beta = 10$.

factor $A_R \equiv A_R^{SD} A_R^{LD}$ associated with anomalous dimension of the relevant baryon-number violating operators. The long-distance factor A_R^{LD} takes a universal value of approximately 1.2, while the short-distance factor A_R^{SD} is highly dependent upon the ultra-violet field content, generally increasing with the addition of new vector-like supermultiplets. For the special cases $(10,\overline{10})$ and $3\times(5,\overline{5})$, where the 1-loop beta-function coefficient of the strong coupling vanishes, a limit for the continuous value of A_R^{SD} may be smoothly numerically extrapolated. The central projected proton lifetime for each of the itemized scenarios is presented in Table I. Current limits on the considered $e^+\pi^0$ decay mode are around 1.7×10^{34} years [35]. Uncertainties in the hadronic matrix element [36], the finite-order renormalization group analysis, the low-energy boundary values, and unknown high-energy threshold effects, coupled with the large powers apparent in Eq. (2) lead to substantial uncertainties in the projected rate, often estimated to exceed an order of magnitude [35]. It would seem then that all scenarios considered in Table I, with the possible exception of the $(10,\overline{10}+5,\overline{5})$ case, are generally consistent with current bounds. Moreover, several of these scenarios point to a high likelihood of a signal at next-generation experiments such as Hyper-Kamiokande [37]. We assume that the potentially dangerous dimension-five higgsino-mediated proton decay has been appropriately suppressed. We remark that this operator is naturally suppressed in the flipped $SU(5)$ GUTs, and the $e^+\pi^0$ lifetime is simultaneously extended by a factor of about five due to absence of $\overline{10}10\overline{10}10$ type contributions [38], although we do not consider those scenarios further here.

III. THE HIGGS BOSON MASS AND VECTOR-LIKE PARTICLES

A. MSSM + $(\mathbf{10}, \overline{\mathbf{10}})$

As previously described, if there is direct coupling among new matter fields and the MSSM Higgs field, the new matter fields will contribute at one-loop level to the CP-even Higgs mass. Here, we consider in detail the case when new vector-like particles fill up $(10, \overline{10})$ dimensional representation of $SU(5)$. The representation $(10, \overline{10})$ of $SU(5)$ decomposes under the MSSM gauge symmetry as follows:

$$\begin{aligned} 10 &= Q_{10}\left(3, 2, \frac{1}{6}\right) + U_{10}\left(\overline{3}, 1, -\frac{2}{3}\right) + E_{10}\,(1, 1, 1)\ , \\ \overline{10} &= \overline{Q}_{10}\left(\overline{3}, 2, -\frac{1}{6}\right) + \overline{U}_{10}\left(3, 1, \frac{2}{3}\right) + \overline{E}_{10}\,(1, 1, -1)\,. \end{aligned} \tag{3}$$

In case when we have new vector-like particles from $(10, \overline{10})$ multiplet, the new couplings $10 \cdot 10 \cdot H_u$ and $\overline{10} \cdot \overline{10} \cdot H_d$ are allowed, analogous to the top–quark Yukawa couplings, but involving the charge $2/3$ ($-2/3$) quark from the 10-plet ($\overline{10}$-plet). Note that we employ the $SU(5)$ notation here for simplicity, with the understanding that H_u and H_d are not complete multiplets of $SU(5)$. Here we assume that the model also contains the SM gauge singlet S field. A new coupling $(S10\overline{10})$ is then allowed.

The part of the superpotential describing interaction among $(10, \overline{10})$, S and the MSSM Higgs fields has the following form:

$$\begin{aligned} W = &\ \kappa_{10} Q_{10}\, U_{10}\, H_u + \kappa'_{10} \overline{Q}_{10}\, \overline{U}_{10}\, H_d + \lambda^Q_{10} S\, \overline{Q}_{10}\, Q_{10} + \lambda^U_{10} S\, \overline{U}_{10}\, U_{10} + \lambda^E_{10} S\, \overline{E}_{10}\, E_{10} \\ &+ \lambda S\, H_u\, H_d + m_S S^2 + M_V\left(\overline{Q}_{10}\, Q_{10} + \overline{U}_{10}\, U_{10} + \overline{E}_{10}\, E_{10}\right), \end{aligned} \tag{4}$$

where we have taken a common vector-like mass at the GUT scale $M_{\rm GUT}$ for simplicity. Thus, the up quark-like pieces of the 10 and $\overline{10}$ acquire Dirac *and* vector-like masses, while the E_{10} lepton-like pieces receive only vector-like masses. We assume that $\kappa_{10} \gg \kappa'_{10}$ because the contribution coming from the coupling κ'_{10} reduces the light Higgs mass in a manner similar to the action of the prominent bottom Yukawa contribution at large tanβ [29]. Also, we require that the $(10, \overline{10})$ fields are R-parity odd. We assume furthermore that mixing of

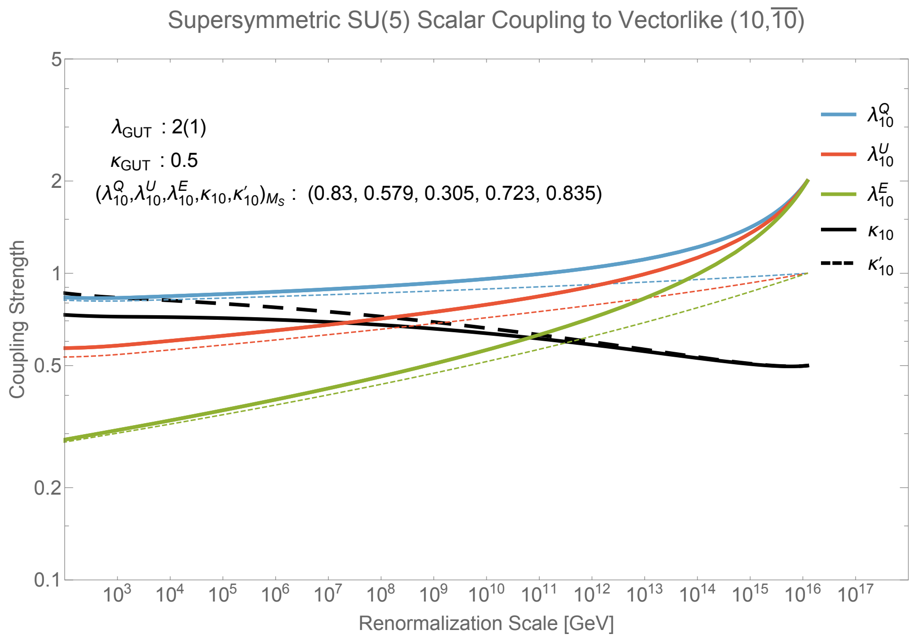

FIG. 2. Renormalization group evolution of the $(10, \overline{10})$ couplings presented in Eq. (4). The κ are analogs of the MSSM Yukawa couplings, linking the vector-like fields to the Higgs. The λ are couplings of vector-like fields and their conjugates to the scalar S.

vector-like particles with the SM are small so as to not violate bounds on flavor changing processes. Nevertheless, even a small mixing of this variety allows vector-like particle from $(10, \overline{10})$ to have prompt decay and avoid cosmological problems.

In Figure 2, we show the renormalization group evolution of the $(10, \overline{10})$ couplings in Eq. (4) from universal boundary values of $\lambda = 2, 1$ and $\kappa = 0.5$ at $M_{\rm GUT}$. In Figure 3, we show the analogous evolution of the $(10, \overline{10})$ vector-like masses in Eq. (4) for a boundary value of $M_{V_{\rm GUT}} = 350$ GeV. A strong fixed-point attraction in the infrared is observed.

Employing the effective potential approach we calculate the additional contribution from the vector-like particles to the CP-even Higgs mass at one loop level. A similar calculation was carried out in Ref. [28].

$$\left[m_h^2\right]_{10} = -M_Z^2 \cos^2 2\beta \left(\frac{3}{8\pi^2} \kappa_{10}^2 t_V \right) + \frac{3}{4\pi^2} \kappa_{10}^4 v^2 \sin^2 \beta \left[t_V + \frac{1}{2} X_{\kappa_{10}} \right], \tag{5}$$

where we have assumed $M_V \gg M_D$ and

$$X_{\kappa_{10}} = \frac{4\widetilde{A}_{\kappa_{10}}^2 \left(3M_S^2 + 2M_V^2\right) - \widetilde{A}_{\kappa_{10}}^4 - 8M_S^2 M_V^2 - 10M_S^4}{6\left(M_S^2 + M_V^2\right)^2} \tag{6}$$

$$t_V = \log\left(\frac{M_S^2 + M_V^2}{M_V^2}\right). \tag{7}$$

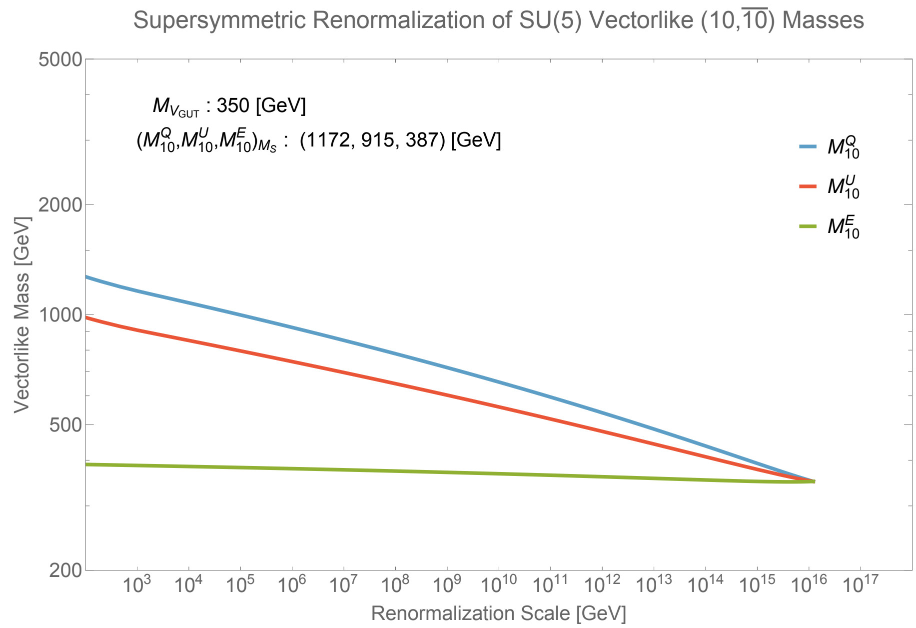

FIG. 3. Renormalization group evolution of the $(10, \overline{10})$ vector-like mass terms presented in Eq. (4).

Here $\widetilde{A}_{\kappa_{10}} = A_{\kappa_{10}} - \mu \cot\beta$, $A_{\kappa_{10}}$ is the $Q_{10} - U_{10}$ soft mixing parameter and μ is the MSSM Higgs bilinear mixing term. $M_{SUSY} \equiv M_S \simeq \sqrt{m_{\tilde{Q}_3} m_{\tilde{U}_3^c}}$, where $m_{\tilde{Q}_3}$ and $m_{\tilde{U}_3^c}$ are the stop left and stop right soft SUSY breaking masses at low scale.

Next, we present the leading 1- and 2- loop contributions to the CP-even Higgs boson mass in the MSSM [30, 31]

$$\begin{aligned}\left[m_h^2\right]_{MSSM} &= M_Z^2 \cos^2 2\beta \left(1 - \frac{3}{8\pi^2}\frac{m_t^2}{v^2} t\right) \\ &+ \frac{3}{4\pi^2}\frac{m_t^4}{v^2}\left[t + \frac{1}{2}X_t + \frac{1}{(4\pi)^2}\left(\frac{3}{2}\frac{m_t^2}{v^2} - 32\pi\alpha_s\right)\left(X_t t + t^2\right)\right],\end{aligned} \tag{8}$$

where

$$t = \log\left(\frac{M_S^2}{M_t^2}\right), \; X_t = \frac{2\widetilde{A}_t^2}{M_S^2}\left(1 - \frac{\widetilde{A}_t^2}{12 M_S^2}\right), \tag{9}$$

with $\widetilde{A}_t = A_t - \mu \cot\beta$, where A_t denotes the left stop and right stop soft mixing parameter.

The light Higgs mass is then expressed as

$$m_h^2 = \left[m_h^2\right]_{MSSM} + \left[m_h^2\right]_{10}. \tag{10}$$

From Eq. (5), we observe that the Higgs mass is very sensitive to the value of κ_{10}, which cannot however be taken arbitrary large without losing perturbativity of the theory up to $M_{\rm GUT}$. We must therefore solve the RGE for κ_{10} to make sure that it remains perturbative

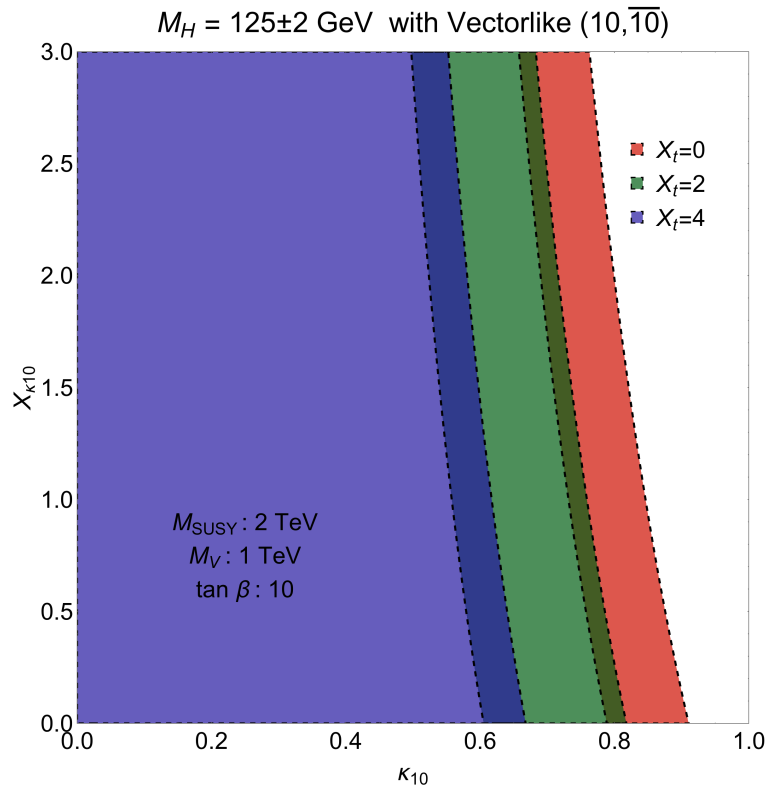

FIG. 4. Regions of the parameter space for κ_{10} of Eq. (4) and $X_{\kappa_{10}}$ of Eq. (6) that are consistent with $m_h = 125 \pm 2$ GeV for various values of X_t from Eq. (9). The darkened regions represent overlap between adjacent bands.

up to the GUT scale. It was shown in Ref. [28] that $\kappa_{10} \approx 1$ can successfully realize a 125 GeV Higgs mass without invoking multi-TeV stop quark masses or a maximal value for the A_t term.

Note that there is an additional tree-level contribution to the CP-even Higgs boson mass from the $\lambda S\, H_u\, H_d$ coupling, given approximately by $\Delta m_h^2 \approx \lambda^2 v^2 \sin^2 2\beta$. Because this contribution is significant only when $\tan\beta \approx 2$, and λ is around $0.5 - 0.7$, we will not not consider this contribution further here.

In Figure 4 we outline the viable parameter regions for κ_{10} and $X_{\kappa_{10}}$, given a Higgs mass of 125 ± 2 GeV, for $M_{\rm SUSY} = 2$ TeV and various values of X_t. We see that the vector particle contribution can be significant, allowing us to find the correct Higgs mass for smaller X_t. The dependency on the $X_{\kappa_{10}}$ term, which depends strongly on the scale of the A-terms, is relatively weak. The much stronger dependency is on the coupling κ_{10}. Typically, for $\kappa_{10} < 1/2$, there is very little boost to the MSSM Higgs mass, although the effect becomes substantial very quickly as this coupling goes to $3/4$ or higher. Smaller couplings are more plausible if the SUSY scale is heavier and/or the vector-like matter scale is lower. Finally, the dependence on $\tan\beta$ is weak.

B. MSSM + $(\mathbf{5}, \overline{\mathbf{5}})$

The representation $(5, \overline{5})$ of $SU(5)$ decomposes under the MSSM gauge symmetry as follows:

$$5 = \overline{L}_5 \left(1, 2, \frac{1}{2}\right) + \overline{D}_5 \left(3, 1, -\frac{1}{3}\right) \ ,$$
$$\overline{5} = L_5 \left(1, 2, -\frac{1}{2}\right) + D_5 \left(\overline{3}, 1, \frac{1}{3}\right) \ . \tag{11}$$

By itself, having only $(5, \overline{5})$ does not allow for any new Yukawa coupling to the MSSM Higgs unless the new states in the $\overline{5}$ are mixed with the usual d^c-quarks and lepton doublets. Such a possibility is very strongly constrained (by flavor violation and unitarity of the CKM matrix, among others), and so we will suppress all such mixings. However, if we introduce an SM gauge singlet S, then Yukawa couplings of the form (in $SU(5)$ notation) $\overline{5} \cdot S \cdot H_u$ and $5 \cdot S \cdot H_d$ are permitted. Here we also introduce a singlet S-field, as in the previous section. In this case the MSSM superpotential has the following additional contribution

$$W \subset \kappa_5 L_5 S H_u + \kappa_5' \overline{L}_5 S H_d + \lambda_5^D S\, \overline{D}_5\, D_5 + \lambda_5^L S\, \overline{L}_5\, L_5 + \lambda S\, H_u\, H_d + m_S S^2 + M_V \left(S\overline{S} + \overline{L}_5 L_5 + \overline{D_5} D_5\right) . \tag{12}$$

We take $\kappa_5 \gg \kappa_5'$ for the same reason mentioned in the previous section. We also assume that there is an additional symmetry forbidding mixing between the vector-like particles and the MSSM matter fields. With this assumption the singlet field S cannot be identified with the right-handed sneutrino.

In Figure 5, we show the renormalization group evolution of the $(10, \overline{10})$ couplings in Eq. (12) from universal boundary values of $\lambda = 2$, 1 and $\kappa = 0.5$ at $M_{\rm GUT}$. In Figure 3, we show the analogous evolution of the $(10, \overline{10})$ vector-like masses in Eq. (12) for a boundary value of $M_{V_{\rm GUT}} = 350$ GeV. A strong fixed-point attraction in the infrared is observed.

Using the effective potential approach we calculate the additional contribution to the CP-even Higgs mass at one loop [28]

$$\left[m_h^2\right]_5 = -M_Z^2 \cos^2 2\beta \left(\frac{1}{8\pi^2}\kappa_5^2 t_V\right) + \frac{1}{4\pi^2}\kappa_5^4 v^2 \sin^2\beta \left[t_V + \frac{1}{2}X_{\kappa_5}\right], \tag{13}$$

where we have assumed $M_V \gg M_D$ and

$$X_{\kappa_5} = \frac{4\widetilde{A}_{\kappa_5}^2 \left(3M_S^2 + 2M_V^2\right) - \widetilde{A}_{\kappa_5}^4 - 8M_S^2 M_V^2 - 10M_S^4}{6\left(M_S^2 + M_V^2\right)^2} \tag{14}$$

$$t_V = \log\left(\frac{M_S^2 + M_V^2}{M_V^2}\right), \tag{15}$$

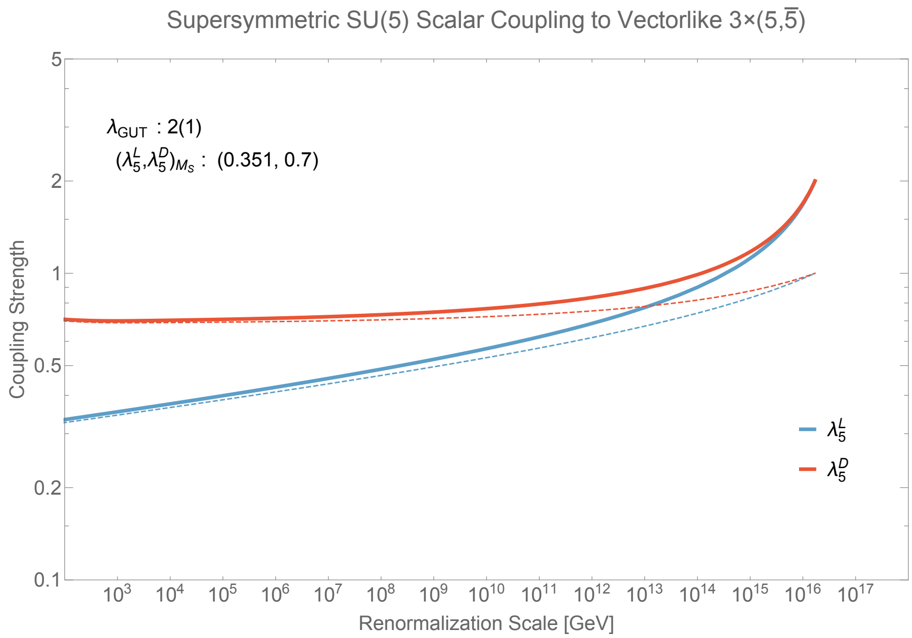

FIG. 5. Renormalization group evolution of the $(5,\overline{5})$ λ couplings presented in Eq. (12), which link the vector-like fields and their conjugates to the scalar S.

with $\widetilde{A}_{\kappa_5} = A_{\kappa_5} - \mu \cot\beta$, where A_{κ_5} is the $L_5 - S$ soft mixing parameter and μ is the MSSM Higgs bilinear mixing term.

In Figure 7 we outline the viable parameter regions for κ_5 and X_{κ_5}, given a Higgs mass of 125 ± 2 GeV, for $M_{\rm SUSY} = 2$ TeV and various values of X_t. We see that the vector particle contribution can be significant and allows us to find the correct Higgs mass for smaller X_t. The previous discussion of Figure 4 carries over.

We also have a similar situation for the MSSM + $(16,\overline{16})$ case, although perturbative gauge coupling unification suggests that the SUSY scale should be pushed upward to several TeV.

IV. NEUTRAL VECTOR-LIKE DOUBLET COMPONENT AS A RESONANCE

In this section we present a new mechanism for the generation of a di-photon excess via resonance of a neutral component of L_5. Following standard notation, we denote the neutral and charged components of L_5 as ν_5 and E_5. Here we assume that we have a $(10,\overline{10}+5,\overline{5})$ set of vector-like particles at low scale. As mentioned above, in order to maintain successful gauge coupling unification in the MSSM vector-like particles should compose full representations of $SU(5)$. On the other hand, gauge coupling unification does not require that all must come from the same representation of $SU(5)$. In particular, in the orbifold GUTs [12–14] and F-theory GUTs [15–18] (See Ref. [19] and references therein.),

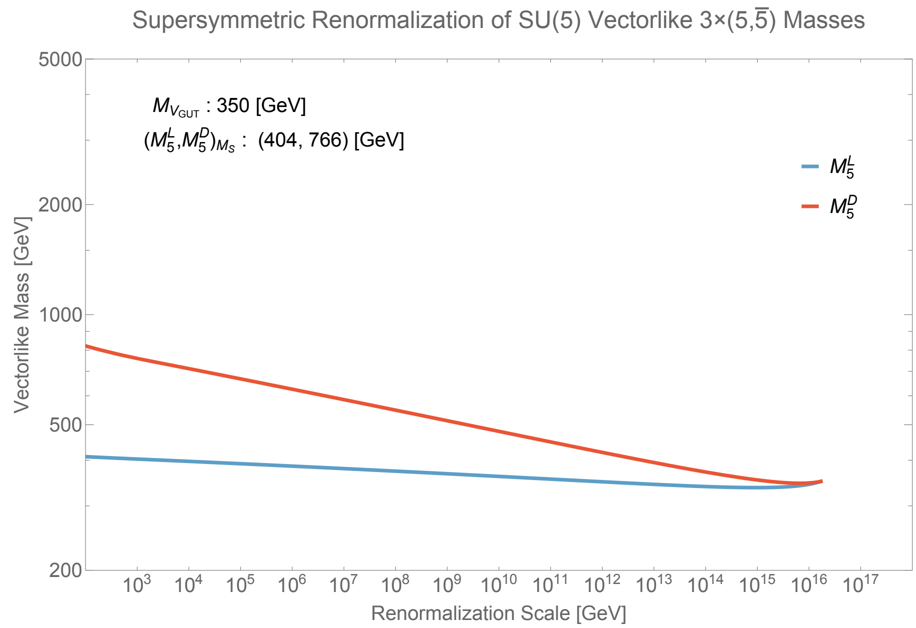

FIG. 6. Renormalization group evolution of the $(5, \bar{5})$ vector-like mass terms presented in Eq. (12).

etc., we can split the multiplets, and then the multiplets in the $(10, \overline{10} + 5, \bar{5})$ can indeed arise from different $SU(5)$ representations.

In order to explain diphoton excess we assume that we have a Z_3 baryon parity [49] in the theory. So in principle the MSSM matter fields will mix with vector like fields. In this framework the relevant couplings to the diphoton excess are the following:

$$W \subset \eta_{ijk} Q_i \, L_j \, D^c_k + \eta^D_{ij5} Q_i \, L_5 \, D^c_j + \eta_1 \, Q_{10} \, L_5 \, D_5 + \eta'_i Q_{10} \, L_i \, D_5 \\ + \eta_i L_5 \, L_i \, E_{10} + \eta_2 L_5 \, H_d \, E_{10}, \tag{16}$$

where the fields with Latin indices are the SM fields. These couplings will lead to the Feynman diagram presented in Figure 8. The first four term in the above equation are relevant for the production, while the fifth term is relevant for the decay of $\tilde{\nu}_5$. The lass term is for mass insertion. Here the MSSM sneutrinos can mix with $\tilde{\nu}_5$ and with appropriate choice of parameters we can have two neutral scalars with very close-by masses which may lead to two nearby resonances. It is interesting to note that in this model we have lepton number violation which can generate proper mass and mixing of the neutrinos[50].

Another way to generate the diagram presented in Fig.8 is to assume that all colored particles $(Q_{10}, \overline{Q}_{10} + U_{10}, \overline{U}_{10} + D_5, \overline{D}_5)$ from $(10, \overline{10} + 5, \bar{5})$ are R-parity odd and all colorless particle $(E_{10}, \overline{E}_{10} + L_5, \overline{L}_5)$ are R-parity even. In this case we need at least two pairs of $(5, \bar{5})$. Then in addition to the interactions given in Eq. 12, we have,

$$W \subset \eta^U_{ijk} Q_i \, \overline{L}^k_5 \, U_j + \eta^D_{ijk} Q_i \, L^k_5 \, D_j + \eta_{kl} L^k_5 \, L^l_5 \, E_{10} + \overline{\eta}_{kl} \overline{L}^k_5 \, \overline{L}^l_5 \, \overline{E}_{10} \\ + \eta_k L^k_5 \, H_d \, E_{10} + \overline{\eta}_k \overline{L}^k_5 \, H_u \, \overline{E}_{10} \ , \tag{17}$$

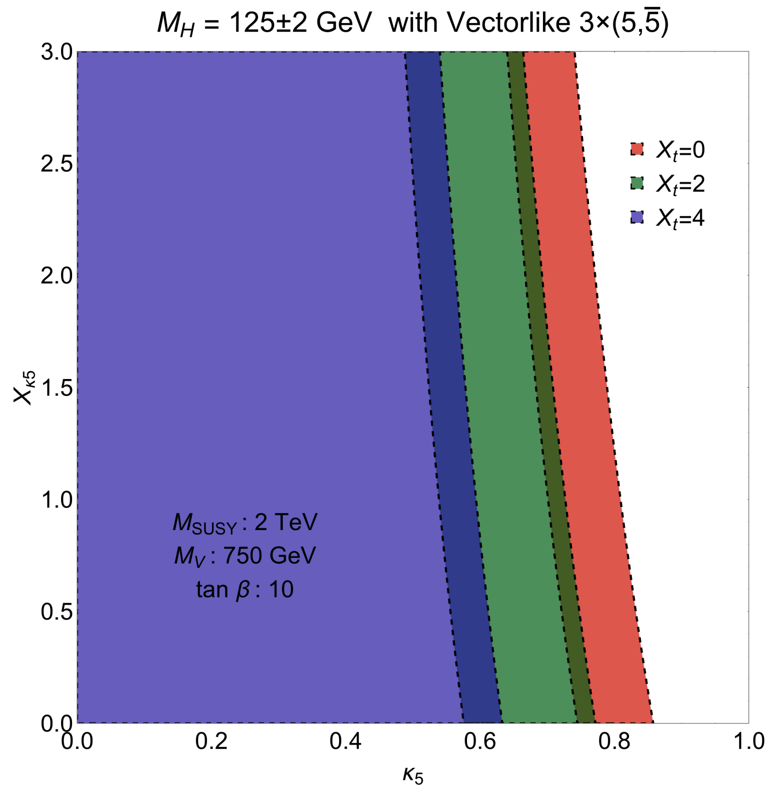

FIG. 7. Regions of the parameter space for κ_5 of Eq. (12) and X_{κ_5} of Eq. (14) that are consistent with $m_h = 125 \pm 2$ GeV for various values of X_t from Eq. (9). The darkened regions represent overlap between adjacent bands.

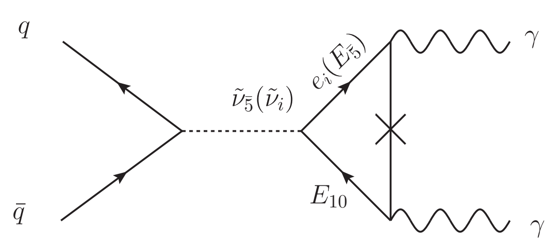

FIG. 8. Production and decay of the neutral component of L_5 via the $Q_{10}L_5D_5$ and $L_5L_5E_{10}$ couplings.

where η_{kl} and $\overline{\eta}_{kl}$ are anti-symmetric in k and l. These couplings can explain the di-photon excess observed at the LHC as follows: the first two operators for productions, the third and fourth operators for decays, and the last two operators for mass insertions. Unlike the previous proposals [24, 25], R-parity is preserved here. Moreover, again with proper choice of parameters we can make L_5^k and $\overline{L}_5^k$ nearly degenerate, and can explain the large decay width around 45 GeV. In this case gauge coupling becomes non-perturbative before 10^{16} GeV. We should point out that this scenario can be embedded nicely into orbifold GUT framework, which we will discuss in a follow-up paper.

V. THE DI-PHOTON EXCESS

	$\kappa_1^{'}$	$\kappa_2^{'}$	$\kappa_3^{'}$		$\kappa_1^{'}$	$\kappa_2^{'}$	$\kappa_3^{'}$
$(Q,\overline{Q})$	$\frac{\lambda_{10}^{Q} g_Y^2}{96\pi^2 M_Q}$	$\frac{3\lambda_{10}^{Q} g_2^2}{32\pi^2 M_Q}$	$\frac{\lambda_{10}^{Q} g_3^2}{8\pi^2 M_Q}$	$(L,\overline{L})$	$\frac{\lambda_5^{L} g_Y^2}{32\pi^2 M_L}$	$\frac{\lambda_5^{L} g_2^2}{32\pi^2 M_L}$	0
$(U,\overline{U})$	$\frac{\lambda_{10}^{U} g_Y^2}{12\pi^2 M_U}$	0	$\frac{\lambda_{10}^{U} g_3^2}{16\pi^2 M_U}$	$(E,\overline{E})$	$\frac{\lambda_5^{E} g_Y^2}{16\pi^2 M_E}$	0	0
$(D,\overline{D})$	$\frac{\lambda_5^{D} g_Y^2}{48\pi^2 M_D}$	0	$\frac{\lambda_5^{D} g_3^2}{16\pi^2 M_D}$				

TABLE II. The coefficients $\kappa_i^{'}$ $(i = 1, 2, 3)$ for different vector-like particles. Note that the effective couplings κ_i can obtained from the above coefficients by multiplying them by the loop functions $A_{1/2}(\tau_F)$ (for $F = Q_{10}, U_{10}, D_5, L_5, E_{10}$) and $A_0(\tau_{\tilde{F}})$ (for SUSY partners of F), presented in Eq. 20

The heavy $F = Q_{10}, U_{10}, D_5, L_5, E_{10}$ fermions, as well as their supersymmetric scalar partners, can induce effective loop-level couplings between S and the SM gauge bosons, as given in Table II. Likewise, couplings to the fermion(s) N can lead to invisible tree-level decays at the collider whenever kinematically allowed,

$$\mathcal{L}_{eff.} = \kappa_1 X B_{\mu\nu} B^{\mu\nu} + \kappa_2 X W^j_{\mu\nu} W^{j\mu\nu} + \kappa_3 X G^a_{\mu\nu} G^{a\mu\nu} + \kappa_{NN} X \overline{N} N, \tag{18}$$

where $B_{\mu\nu}$, $W^j_{\mu\nu}$ and $G^a_{\mu\nu}$ represents the field strength tensor of the SM gauge bosons of the $U(1)_Y$, $SU(2)_L$ and $SU(3)_c$ groups, respectively, with $j = 1, 2, 3$ and $a = 1, 2, ..8$ are the indices of the adjoint representations of $SU(2)_L$ and $SU(3)_c$ respectively. The effective couplings κ_i $(i = 1, 2, 3)$ can be obtained from the coefficients $\kappa_i^{'}$ presented in Table II by,

$$\kappa_i = \kappa_i^{'} \left(A_{1/2}(\tau_F) + \frac{A_F}{M_{\tilde{F}}} A_0(\tau_{\tilde{F}}) \right), \tag{19}$$

where A_F are the trilinear couplings of S with the SUSY partners of the vector-like fermions. The loop functions $A_{1/2}(\tau)$ and $A_0(\tau)$ with $\tau = 4M^2/M_S^2$ are given by,

$$\begin{aligned} A_{1/2}(\tau) &= 2\tau[1 + (1-\tau) f(\tau)] \,, \\ A_0(\tau) &= -\tau + \tau^2 f(\tau) \,, \end{aligned} \tag{20}$$

with

$$f(x) = \begin{cases} \arcsin^2[1/\sqrt{x}], & \text{if } x \geq 1 \\ -\frac{1}{4}[\ln \frac{1+\sqrt{1-x}}{1-\sqrt{1-x}} - i\pi]^2, & \text{if } x < 1. \end{cases} \tag{21}$$

After rotation to the physical gauge boson states, these effective couplings can be written for both isosinglet and $SU(2)_L$ doublet as,

$$\begin{aligned}
\kappa_{\gamma\gamma} &= \kappa_1 \cos^2\theta_W + \kappa_2 \sin^2\theta_W \,, \\
\kappa_{ZZ} &= \kappa_2 \cos^2\theta_W + \kappa_1 \sin^2\theta_W \,, \\
\kappa_{Z\gamma} &= (\kappa_2 - \kappa_1) \sin 2\theta_W \,, \\
\kappa_{WW} &= 2\kappa_2 \,, \\
\kappa_{gg} &= \kappa_3 \,,
\end{aligned} \tag{22}$$

where θ_W is the weak mixing angle.

The current LHC bounds on vector-like quark masses range from 735 GeV for D-type isosinglets to 855 GeV for the doublet Q (see [32] and references therein). The loop contribution from charged sfermions interfere constructively with that from fermions. For simplicity, we assume a common mass for the heavy fermions and their superpartners, $M_F = M_{\tilde{F}}$, during the evaluation of loop functions. With a reasonable choice of $A_F/M_{\tilde{F}} \approx 3$, including the sfermions enhances $\kappa_{\gamma\gamma}$ and κ_{gg} by a factor of ~ 2 in comparison with non-MSSM cases.

The evolution of the couplings and masses of vector-like fermions between the GUT scale and the scale of the observed resonance $M_S \sim 750$ GeV are presented in Table III for both $(10,\overline{10})$ and $(5,\overline{5})$ extensions of the MSSM. We find that at least three copies of $(5,\overline{5})$ vector-like multiplets are needed in order to enhance the scalar resonance cross-section to fit the data. Four copies of $(5,\overline{5})$ provide comparatively better fit to the data, although this scenario, like the $(16,\overline{16})$ is on the edge of criticality and may exhibit a Landau pole if the vector-like and/or SUSY scales are too light. Similarly, two copies of $(10,\overline{10})$ multiplets fit the excess better than one copy, although this scenario is strictly incompatible with perturbative unification.

	Masses [GeV]	Couplings
MSSM + $(10,\overline{10})$	$M_{10}^Q = 1172$, $M_{10}^U = 915$, $M_{10}^E = 387$	$\lambda_{10}^Q = 0.830$, $\lambda_{10}^U = 0.579$, $\lambda_{10}^E = 0.305$
MSSM + $3 \times (5,\overline{5})$	$M_5^L = 404$, $M_5^D = 766$	$\lambda_5^L = 0.351$, $\lambda_5^D = 0.700$

TABLE III. Renormalized vector-like fermion couplings and masses at 750 GeV.

At the LHC, the diphoton production cross-section can be written in the narrow-width approximation,

$$\sigma_{\gamma\gamma} = \frac{K\,\pi^2}{8M_S} \frac{\Gamma(S\to gg)\Gamma(S\to\gamma\gamma)}{\Gamma_S} \times \frac{1}{s} \int dx_1 dx_2 f_g(x_1) f_g(x_2) \delta\left(x_1 x_2 - \frac{M_S^2}{s}\right), \tag{23}$$

where f_g is the gluon parton distribution function inside a proton, x denotes the fraction of each beam's energy carried away by the corresponding gluon, K is the QCD K-factor and

$\sqrt{s} = 13$ TeV. $\Gamma_S = \Gamma_{\gamma\gamma} + \Gamma_{Z\gamma} + \Gamma_{ZZ} + \Gamma_{WW} + \Gamma_{gg} + \Gamma_{N\overline{N}}$ denotes the total decay width of S. We have used the PDFs of `MSTW2008NNLO` [39] for the gluon luminosity calculation with the factorization scale set at M_S. We used the K-factor of 1.98 in our calculation, which is the K-factor for 750 GeV SM-like Higgs [40].

We should emphasize here that the experimentally observed width of the resonance is quite large. ATLAS reported a width as large as $\Gamma = 0.06 M_S$. However the data collected so far is insufficient to claim such a broad width conclusively. Ref. [11] has performed a likelihood analysis to fit both CMS and ATLAS data and checked for their consistency against the 8 TeV data as well. Their fit to the combined run-I and run-II data indicates that the resonance at 750 GeV can be fit by $\sigma_{\gamma\gamma} \sim 0.7 - 16$ fb for $\Gamma_S \sim 5 - 100$ GeV at 2σ level. Nevertheless, we adopt a conservative point of view and take the indicated width at face value, thus restricting our study to $\Gamma_S \sim 5 - 45$ GeV.

It should be noted that the loop induced diphoton and dijet widths are inadequate to account for $\mathcal{O}(10)$ GeV width. Consequently, we require the width $\Gamma_{N\overline{N}}$ to be significant. In Table IV, we show the benchmark points for each unification scheme that explains the diphoton excess, and the cross-sections into several leading associated final states.

		Γ_S [GeV]	$\sigma_{\gamma\gamma}$ [fb]	σ_{ZZ} [fb]	$\sigma_{Z\gamma}$ [fb]	σ_{WW} [fb]	σ_{gg} [fb]	$\sigma_{N\overline{N}}$ [fb]
MSSM + $(10, \overline{10})$	BP-1	5	1.57	2.08	0.08	4.90	985	7013
	BP-2	8	0.98	1.30	0.05	3.05	614	7388
MSSM + $3 \times (5, \overline{5})$	BP-3	5	7.04	15.2	2.41	41.2	3838	11891
	BP-4	25	1.40	3.04	0.48	8.22	766	15015

TABLE IV. Total decay width of S and cross-section in associated final states. The invisible cross-section $\sigma_{N\overline{N}}$ is used to evaluate its monojet signal rate. The couplings and masses of vector-like fermions used are shown in Table III.

In Table IV, BP-1 and BP-3 show the values of cross-sections in different channels if we fit $\Gamma_S \approx 5$ GeV for different unification schemes. Using the results of Ref. [11], we notice that $\sigma_{\gamma\gamma}$ for BP-3 is higher than the 2σ upper limit of cross-section that is needed to fit a width of 5 GeV. In contrast, BP-2 and BP-4 represent the highest Γ_S that can be fit with the allowed 2σ lower limit on the corresponding cross-section of Ref. [11], with the masses and couplings of $(10, \overline{10})$ and $3 \times (5, \overline{5})$ respectively. Clearly, the BPs belonging to$(10, \overline{10})$ are almost at the 2σ lower edge of the cross-section range of interest. In contrast, a relatively wider range of width can be satisfied with appreciable cross-section for the $3 \times (5, \overline{5})$ cases.

Next, let us discuss the constraints from few associated diboson ($S \to W^+W^-$, ZZ, $Z\gamma$) final states, which arise from the couplings presented in Eq. 18. The W^+W^-, ZZ, $Z\gamma$ signals are estimated to be at comparable rate to $\gamma\gamma$ channel as they originate from the same set of couplings, as shown in Table IV. Among these three weak-boson channels, $Z\gamma$ is the most stringent and CMS [41] constrains a monophoton signal to be less than 30 fb with missing energy $\not{E}_T > 250$ GeV. The supersymmetric $(10, \overline{10})$ and $(5, \overline{5})$ cases we considered here clearly satisfy these bounds.

Since the gg and $\overline{N}N$ can take up sizeable partial width in comparison to $\gamma\gamma$, they should be investigated more thoroughly. In their most recent dijet analysis, using 13 TeV data, both CMS [42] and ATLAS [43] set a bound on dijet resonance mass only above 1 TeV. However, CMS places a 2 pb bound on a 750 GeV gg resonance from run-1 data [9]. From this result we can easily estimate a model independent bound on the relative ratio between gg and $\gamma\gamma$,

$$\frac{\mathrm{BR}_{gg}}{\mathrm{BR}_{\gamma\gamma}} < \eta \cdot \frac{\sigma_{jj}^{8\mathrm{TeV}}}{\sigma_{\gamma\gamma}} , \tag{24}$$

where $\eta = \sigma^S_{13\mathrm{TeV}}/\sigma^S_{8\mathrm{TeV}} \approx 5$ accounts for the difference in the S production cross-section at 8 TeV. This constraint can rule out heavy quark only models where the two gluon channel dominates over diphoton due to quarks' fractional electric charges. In our unification models, the inclusion of heavy leptons in $10 + \overline{10}$ and $5 + \overline{5}$ enhances $\kappa_{\gamma\gamma}$ and becomes consistent with this dijet constraint. The dijet cross-sections of our BPs at 8 TeV, in comparison with the same at 13 TeV, are shown in Table V.

BP	$\sigma_{gg}^{13\ \mathrm{TeV}}$ [fb]	$\sigma_{gg}^{8\ \mathrm{TeV}}$ [fb]
BP-1	985	210
BP-2	614	131
BP-3	3838	818
BP-4	766	163

TABLE V. Comparison of dijet cross-section of our BPs at 8 TeV and 13 TeV. The CMS 8 TeV bound on cross-section at 750 GeV dijet invariant mass is 2 pb (for gg resonance) [9].

Also relevant to the dijet constraints, we should discuss the case where the neutral component of vector-like doublets ($\tilde{\nu}_5$) act as the resonance. In this case $\tilde{\nu}_5$(s) are produced by tree-level interactions with valence quarks, as shown in Fig. 8. Hence, it can potentially decay to $q\bar{q}$ with a large cross-section. These scenarios severely constrained by CMS dijet bounds [9]. In addition, the charged scalar of the doublet will also contribute to the dijet with an even larger cross-section at about the same invariant mass [25]. To evade this bound we require η couplings relevant to the interactions of the sneutrinos with SM quarks to be $\lesssim 0.1$. However, this results in an appreciable decrease in the width of the resonance. We will discuss about possible ways to resolve this problem in the Sub-section V B.

Coming back to SM singlet scalar resonance, we notice from Table IV, the invisible decay, $S \to \overline{N}N$, takes up the major fraction of the total width. This channel is associated with a monojet jet process, $pp \to Sj \to j + \not{E}_T$, where an extra jet from initial state radiation, or gluon-splitting, can provide a large transverse momentum and boost the invisibly decayed S into missing transverse energy. The monojet cross-section can be written as,

$$\sigma_{\overline{N}Nj}(p_T) = \epsilon_{p_T} \times \left(\sigma^{\text{obs.}}_{\gamma\gamma} \cdot \frac{\text{BR}_{\overline{N}N}}{\text{BR}_{\gamma\gamma}} \right) , \tag{25}$$

where ϵ_{p_T} is the cross-section ratio between $pp \to Sj$ with jet transverse momentum p_T harder than a given threshold to $pp \to S$.

$$\sigma_{\overline{N}Nj}(p_T) \equiv \sigma_S \times \text{BR}_{\overline{N}N} \times \epsilon_{p_T} \tag{26}$$

We obtain ϵ_{p_T} for various thresholds, as given in Table VI. For monojet events, this jet p_T equals the missing transverse energy $\not{E}_T$.

$\not{E}_T$ cut (GeV)	ϵ_{p_T} (8 TeV)	ϵ_{p_T} (13 TeV)	CMS [44] 8 TeV bound at 95% C.L.
200	0.14	0.18	
300	0.063	0.094	0.09 pb
400	0.031	0.052	
500	0.015	0.030	0.006 pb

TABLE VI. Parton level ϵ_{p_T} for monojet events with resonance at 750 GeV. MadGraph/MadEvent [46] is used to simulate the monojet events. The production cross-section σ_S is a factor of 5 smaller at the 8 TeV run.

It is also interesting to note that the monojet cross-section falls faster than the CMS constraint, and a higher $\not{E}_T$ cut gives a better constraint. Taking the upper limit with $\not{E}_T > 500$ GeV, the invisible decay branching is constrained to be,

$$\frac{\text{BR}_{\gamma\gamma}}{\text{BR}_{\overline{N}N}} > \eta^{-1} \cdot \frac{\epsilon_{p_T}\ \sigma_{\gamma\gamma}}{0.006\text{pb}} \sim 10^{-3} \text{ @ } 95\%\text{C.L}, \tag{27}$$

This constraint may be in tension with a large invisible width, which the measured $6\% M_S$ often requires. In the next sub-section, we discuss options to evade this monojet constraint.

A. Semi-invisible S decays

As a large invisible width in the S decay may be constrained by monojet limits, it can be worth promoting such invisible $\overline{N}N$ final state into 'semi-'invisible, by allowing N to decay into another missing particle and relatively soft leptons arising dominantly from Z^* decay with $10-20$ GeV energy due to small mass gaps between N and the missing particle. The leptons can also be due to a slepton in between the NLSP and LSP. Because the monojet search veto isolated leptons (e, μ) with a small p_T (>7 GeV at CMS [44] and $>$ 10 GeV at ATLAS [45]) and $p_T(\tau_h) > 20$ GeV, the leptons in the semi-visible decays cannot be vetoed during monojet search, thus evading such bounds. The direct production (without monojet) from the resonance channel produces N's back-to-back and only soft leptons exist in the final state without any missing energy.

Via the MSSM framework of our benchmark scenarios, the supersymmetric partner of S itself can well serve this purpose. For example, a $\kappa_S S^3$ type of term in the superpotential, as in the popular Next-to MSSM (NMSSM) [47] model, allows the singlet decay into a pair of singlinos, and the singlino can mix with other gauginos and Higgsinos in the model. As the singlino can derive its mass separately when the singlet develops its own vacuum expectation value, the singlino can have mass split of around $10-30$ GeV with Higgsinos and bino, with the latter being the dominant component of the LSP, while the singlino dominates the NLSP. Also, one can think of a slepton in-between the NLSP and the LSP, $\tilde{\chi}^0_2 \to \tilde{\chi}^0_1 ll$ where the lepton energies depend on the mass gap between slepton and the $\tilde{\chi}^0$s.

In such a singlino-gaugino-Higgsino mixed case, a large self-coupling $\kappa_S \sim 1$ can dominate the S width by decaying into a pair of singlino-dominated NLSPs, which in turn produce high enough p_T leptons to evade monojet searches. Note that, beside the cubic κS^3 term, the $\lambda_S S H_u H_d$ term also allows S decay into neutrinos via their mixing with MSSM Higgses. However, this interaction can induce $S \to VV, hh$ at branching ratios comparable to that into neutrinos, which are highly constrained by four lepton/b-jet searches.

B. The $\tilde{\nu}_5$ resonance case

As mentioned earlier in this section that the $\tilde{\nu}_5$ resonance scenarios, discussed in the Section IV, also suffer from the narrow width problem. One way the narrow width problem is resolved if the neutral scalar from the doublet predominantly decays with a broad width into a wino-type chargino and soft lepton with $p_T \sim 10-40$ GeV (or even larger), which depends on the mass gap between the sneutrino and chargino. The nature of the lepton depends on the exact nature of the interaction. We assume that the LSP is not pure wino but contain sufficient bino and/or higgsino component, so that the mass gap between the chargino and the LSP is large enough to not being ruled out by long-lived charged particle searches. Hence the final state then will be monolepton plus missing energy. The current CMS monolepton search [48] triggers on $E_T(e) > 80$ GeV and $p_T(\mu) > 40$ GeV. If the resonance width is relatively small, $\Gamma_{\tilde{\nu}_5}$ ~5 GeV, a sneutrino-chargino mass gap of $\sim$ 50

GeV can evade the monojet bound and only leads to a few percent of $\tilde{\nu}_5 \to e^- \tilde{\chi}^+$ events with lepton $p_T > 80$ GeV. For the scenarios discussed in the Section IV, it means that a sub-picobarn monolepton cross-section with missing energy around $100 - 200$ GeV is thus consistent with both monojet and monolepton searches. The sneutrino-chargino mass gap should remain below the monolepton threshold. However, for a large width $\Gamma = 6\% M_S$, the closeness of sneutrino and chargino masses is not sufficient to suppress virtual $\tilde{\nu}_5$ processes. The virtual $\tilde{\nu}_5$ processes yield a large number of leptons with enough energy to be seen in lepton(s)+$\not{E}_T$ channels, and can easily be in tension with or constrained by these searches.

Admittedly this problem can also be resolved if more than one sneutrinos are near-degenerate with mass splitting of $\mathcal{O}(10)$ GeV. Due to the antisymmetric nature of the $10\bar{5}\bar{5}$ couplings either $\tilde{\nu}_5$ mixes with MSSM sneutrinos (for the superpotential of Eq. 16) or we require at least two L_5 doublets (for the superpotential of Eq. 17). Hence it is natural to have two very close-by scalar resonances. If this is the correct interpretation of the observed bump, then with additional data it will resolve into two isolated narrow resonances.

VI. CONCLUSION

In conclusion, we considered vector-like multiplets $(5, \overline{5})$ and $(10, \overline{10})$ in the context of $SU(5)$ gauge coupling unification and investigated their compatibility with the 750 GeV diphoton resonance using the renormalized masses and Yukawa couplings at that scale. We demonstrated the effect of these new multiplets on the unified scale and coupling strength. We also investigated the new Yukawa couplings and mass terms associated with new vector-like multiplets and the new scalar perturbatively, evolving down universal values from the GUT scale. The presence of the new vector-like multiplets allow us to reduce the burden on the stop squarks to provide the additional necessary contribution to the 125 GeV Higgs mass in MSSM. We also showed that the proton decay rate for $p \to e^+ \pi^0$ in these models may be enhanced and lie within the reach of future proton decay experiments.

We showed the capacity of 3 copies of $(5, \overline{5})$ and 1 copy of $(10, \overline{10})$ to explain the observed excess. However, the width associated with such a resonance is very narrow ~ 0.6 GeV and 1.24 GeV for $(5, \overline{5})$ and $(10, \overline{10})$ respectively, whereas the experimentally preferred width is much larger. In order to accommodate such a width we introduced an additional decay mode where the new scalar singlet decays into singlinos, which, in turn, decay into Higgsinos by emitting soft leptons with $p_T \sim 10 - 20$ GeV. This scenario is not excluded by monojet or other constraints.

In addition, we also showed that using components from different multiplets of $(10, \overline{10})$ and $(5, \overline{5})$ (without gauge coupling unification), we can write down a new interaction where the neutral component of the new lepton doublet scalar is responsible for the resonance. In such a scenario, R-parity is preserved. The decay width can be enhanced by decay modes associated with scalar decay into a soft lepton and chargino, which is nearly-degenerate with the LSP. However, it is also possible to have two new L_5 doublets or mixing between one L_5 doublet and MSSM doublets L_i due to the antisymmetric nature of the coupling $10\bar{5}\bar{5}$. In such a case, we can have two adjacent resonances, and no additional contribution to the width is required.

ACKNOWLEDGMENTS

We thank Teruki Kamon for helpful discussions. This work is supported in part by DOE grant numbers DE-FG02-13ER42020 (B.D., T.G.) and doe-sc0013880 (Q.S.), Natural Science Foundation of China grant numbers 11135003, 11275246, and 11475238 (T.L), National Science Foundation grant number PHY-1521105 (J.W.W.), and the Mitchell Institute for Fundamental Physics and Astronomy (Y.G.).

---

[1] G. Aad *et al.* [ATLAS Collaboration], Phys. Lett. B **716**, 1 (2012) [arXiv:1207.7214 [hep-ex]].

[2] S. Chatrchyan *et al.* [CMS Collaboration], Phys. Lett. B **716**, 30 (2012) [arXiv:1207.7235 [hep-ex]].

[3] For a review, see K. R. Dienes, Phys. Rept. **287**, 447 (1997).

[4] K.S. Babu and J.C. Pati, Phys. Lett. B **384**, 140 (1996); C. Kolda and J. March-Russell, Phys. Rev. D **55**, 4252 (1997); M. Bastero-Gil and B. Brahmachari, Nucl. Phys. B **575**, 35 (2000); J.L. Chkareuli, I. Gogoladze and A.B. Kobakhidze, Phys. Rev. Lett. **80**, 912 (1998); J.L. Chkareuli, C.D. Froggatt, I. Gogoladze and A.B. Kobakhidze, Nucl. Phys. B **594**, 23 (2001).

[5] ATLAS note, ATLAS-CONF-2015-081, "Search for resonances decaying to photon pairs in 3.2 fb−1 of pp collisions at $\sqrt{s} = 13$ TeV with the ATLAS detector".

[6] CMS note, CMS PAS EXO-15-004, "Search for new physics in high mass diphoton events in proton-proton collisions at 13 TeV".

[7] V. Khachatryan *et al.* [CMS Collaboration], Phys. Lett. B **750**, 494 (2015) [arXiv:1506.02301 [hep-ex]].

[8] G. Aad *et al.* [ATLAS Collaboration], Phys. Rev. Lett. **113**, no. 17, 171801 (2014) [arXiv:1407.6583 [hep-ex]].

[9] CMS Collaboration [CMS Collaboration], CMS-PAS-EXO-14-005.

[10] B. Dutta, Y. Gao, T. Ghosh, I. Gogoladze and T. Li, arXiv:1512.05439 [hep-ph].

[11] A. Falkowski, O. Slone and T. Volansky, arXiv:1512.05777 [hep-ph].

[12] Y. Kawamura, Prog. Theor. Phys. **103** (2000) 613; Prog. Theor. Phys. **105**(2001)999; Theor. Phys. **105**(2001)691.

[13] G. Altarelli and F. Feruglio, Phys. Lett. B **511**, 257 (2001).

[14] L. Hall and Y. Nomura, Phys. Rev. D **64**, 055003 (2001).

[15] R. Donagi and M. Wijnholt, arXiv:0802.2969 [hep-th].

[16] C. Beasley, J. J. Heckman and C. Vafa, JHEP **0901**, 058 (2009).

[17] C. Beasley, J. J. Heckman and C. Vafa, JHEP **0901**, 059 (2009).

[18] R. Donagi and M. Wijnholt, arXiv:0808.2223 [hep-th].

[19] T. Li and D. V. Nanopoulos, JHEP **1110**, 090 (2011) [arXiv:1005.3798 [hep-ph]].

[20] K. Harigaya and Y. Nomura, arXiv:1512.04850 [hep-ph]; Y. Mambrini, G. Arcadi and A. Djouadi, arXiv:1512.04913 [hep-ph]; M. Backovic, A. Mariotti and D. Redigolo, arXiv:1512.04917 [hep-ph]; A. Angelescu, A. Djouadi and G. Moreau, arXiv:1512.04921 [hep-ph]; Y. Nakai, R. Sato and K. Tobioka, arXiv:1512.04924 [hep-ph]; S. Knapen, T. Melia, M. Papucci and K. Zurek, arXiv:1512.04928 [hep-ph]; D. Buttazzo, A. Greljo and D. Marzocca, arXiv:1512.04929 [hep-ph]; A. Pilaftsis, arXiv:1512.04931 [hep-ph]; R. Franceschini *et al.*, arXiv:1512.04933 [hep-ph]; S. Di Chiara, L. Marzola and M. Raidal, arXiv:1512.04939 [hep-ph].

[21] S. D. McDermott, P. Meade and H. Ramani, arXiv:1512.05326 [hep-ph]; R. Benbrik, C. H. Chen and T. Nomura, arXiv:1512.06028 [hep-ph]; J. Ellis, S. A. R. Ellis, J. Quevillon, V. Sanz and T. You, arXiv:1512.05327 [hep-ph]; M. Low, A. Tesi and L. T. Wang, arXiv:1512.05328 [hep-ph]; B. Bellazzini, R. Franceschini, F. Sala and J. Serra, arXiv:1512.05330 [hep-ph]; R. S. Gupta, S. Jger, Y. Kats, G. Perez and E. Stamou, arXiv:1512.05332 [hep-ph]; C. Petersson and R. Torre, arXiv:1512.05333 [hep-ph]; E. Molinaro, F. Sannino and N. Vignaroli, arXiv:1512.05334 [hep-ph]; Q. H. Cao, Y. Liu, K. P. Xie, B. Yan and D. M. Zhang, arXiv:1512.05542 [hep-ph]; S. Matsuzaki and K. Yamawaki, arXiv:1512.05564 [hep-ph]; A. Kobakhidze, F. Wang, L. Wu, J. M. Yang and M. Zhang, arXiv:1512.05585 [hep-ph]; R. Martinez, F. Ochoa and C. F. Sierra, arXiv:1512.05617 [hep-ph]; P. Cox, A. D. Medina, T. S. Ray and A. Spray, arXiv:1512.05618 [hep-ph]; D. Becirevic, E. Bertuzzo, O. Sumensari and R. Z. Funchal, arXiv:1512.05623 [hep-ph]; J. M. No, V. Sanz and J. Setford, arXiv:1512.05700 [hep-ph]; S. V. Demidov and D. S. Gorbunov, arXiv:1512.05723 [hep-ph]; W. Chao, R. Huo and J. H. Yu, arXiv:1512.05738 [hep-ph]; S. Fichet, G. von Gersdorff and C. Royon, arXiv:1512.05751 [hep-ph]; D. Curtin and C. B. Verhaaren, arXiv:1512.05753 [hep-ph]; L. Bian, N. Chen, D. Liu and J. Shu, arXiv:1512.05759 [hep-ph]; J. Chakrabortty, A. Choudhury, P. Ghosh, S. Mondal and T. Sri-

vastava, arXiv:1512.05767 [hep-ph]; A. Ahmed, B. M. Dillon, B. Grzadkowski, J. F. Gunion and Y. Jiang, arXiv:1512.05771 [hep-ph]; C. Csaki, J. Hubisz and J. Terning, arXiv:1512.05776 [hep-ph]; D. Aloni, K. Blum, A. Dery, A. Efrati and Y. Nir, arXiv:1512.05778 [hep-ph]; Y. Bai, J. Berger and R. Lu, arXiv:1512.05779 [hep-ph]; E. Gabrielli, K. Kannike, B. Mele, M. Raidal, C. Spethmann and H. Veerme, arXiv:1512.05961 [hep-ph]; J. S. Kim, J. Reuter, K. Rolbiecki and R. R. de Austri, arXiv:1512.06083 [hep-ph]; A. Alves, A. G. Dias and K. Sinha, arXiv:1512.06091 [hep-ph]; E. Megias, O. Pujolas and M. Quiros, arXiv:1512.06106 [hep-ph]; L. M. Carpenter, R. Colburn and J. Goodman, arXiv:1512.06107 [hep-ph]; J. Bernon and C. Smith, arXiv:1512.06113 [hep-ph]; W. Chao, arXiv:1512.06297 [hep-ph]; M. T. Arun and P. Saha, arXiv:1512.06335 [hep-ph]; C. Han, H. M. Lee, M. Park and V. Sanz, arXiv:1512.06376 [hep-ph]; S. Chang, arXiv:1512.06426 [hep-ph]; I. Chakraborty and A. Kundu, arXiv:1512.06508 [hep-ph]; H. Han, S. Wang and S. Zheng, arXiv:1512.06562 [hep-ph]; X. F. Han and L. Wang, arXiv:1512.06587 [hep-ph]; F. Wang, L. Wu, J. M. Yang and M. Zhang, arXiv:1512.06715 [hep-ph]; J. Cao, C. Han, L. Shang, W. Su, J. M. Yang and Y. Zhang, arXiv:1512.06728 [hep-ph]; F. P. Huang, C. S. Li, Z. L. Liu and Y. Wang, arXiv:1512.06732 [hep-ph]; J. J. Heckman, arXiv:1512.06773 [hep-ph]; X. J. Bi, Q. F. Xiang, P. F. Yin and Z. H. Yu, arXiv:1512.06787 [hep-ph]; J. S. Kim, K. Rolbiecki and R. R. de Austri, arXiv:1512.06797 [hep-ph]; J. M. Cline and Z. Liu, arXiv:1512.06827 [hep-ph]; M. Chala, M. Duerr, F. Kahlhoefer and K. Schmidt-Hoberg, arXiv:1512.06833 [hep-ph]; S. M. Boucenna, S. Morisi and A. Vicente, arXiv:1512.06878 [hep-ph]; P. S. B. Dev and D. Teresi, arXiv:1512.07243 [hep-ph]; J. de Blas, J. Santiago and R. Vega-Morales, arXiv:1512.07229 [hep-ph]; C. W. Murphy, arXiv:1512.06976 [hep-ph]; U. K. Dey, S. Mohanty and G. Tomar, arXiv:1512.07212 [hep-ph]; G. M. Pelaggi, A. Strumia and E. Vigiani, arXiv:1512.07225 [hep-ph]; W. C. Huang, Y. L. S. Tsai and T. C. Yuan, arXiv:1512.07268 [hep-ph]; Q. H. Cao, S. L. Chen and P. H. Gu, arXiv:1512.07541 [hep-ph]; S. Chakraborty, A. Chakraborty and S. Raychaudhuri, arXiv:1512.07527 [hep-ph]; W. Altmannshofer, J. Galloway, S. Gori, A. L. Kagan, A. Martin and J. Zupan, arXiv:1512.07616 [hep-ph]; M. Cveti, J. Halverson and P. Langacker, arXiv:1512.07622 [hep-ph]; K. Das and S. K. Rai, arXiv:1512.07789 [hep-ph]; K. Cheung, P. Ko, J. S. Lee, J. Park and P. Y. Tseng, arXiv:1512.07853 [hep-ph]; J. Liu, X. P. Wang and W. Xue, arXiv:1512.07885 [hep-ph]; J. Zhang and S. Zhou, arXiv:1512.07889 [hep-ph]; G. Li, Y. n. Mao, Y. L. Tang, C. Zhang, Y. Zhou and S. h. Zhu, arXiv:1512.08255 [hep-ph]; M. Son and A. Urbano, arXiv:1512.08307 [hep-ph]; H. An, C. Cheung and Y. Zhang, arXiv:1512.08378 [hep-ph]; F. Wang, W. Wang, L. Wu, J. M. Yang and M. Zhang, arXiv:1512.08434 [hep-ph]; Q. H. Cao, Y. Liu, K. P. Xie, B. Yan and D. M. Zhang, arXiv:1512.08441 [hep-ph]; J. Gao, H. Zhang and

H. X. Zhu, arXiv:1512.08478 [hep-ph]; F. Goertz, J. F. Kamenik, A. Katz and M. Nardecchia, arXiv:1512.08500 [hep-ph]; P. S. B. Dev, R. N. Mohapatra and Y. Zhang, arXiv:1512.08507 [hep-ph]; Y. L. Tang and S. h. Zhu, arXiv:1512.08323 [hep-ph]; J. Cao, F. Wang and Y. Zhang, arXiv:1512.08392 [hep-ph]; C. Cai, Z. H. Yu and H. H. Zhang, arXiv:1512.08440 [hep-ph]; W. Chao, arXiv:1512.08484 [hep-ph]; N. Bizot, S. Davidson, M. Frigerio and J.-L. Kneur, arXiv:1512.08508 [hep-ph]; L. E. Ibanez and V. Martin-Lozano, arXiv:1512.08777 [hep-ph]; Y. Hamada, T. Noumi, S. Sun and G. Shiu, arXiv:1512.08984 [hep-ph]; S. K. Kang and J. Song, arXiv:1512.08963 [hep-ph]; S. Kanemura, K. Nishiwaki, H. Okada, Y. Orikasa, S. C. Park and R. Watanabe, arXiv:1512.09048 [hep-ph]; Y. Jiang, Y. Y. Li and T. Liu, arXiv:1512.09127 [hep-ph]; K. Kaneta, S. Kang and H. S. Lee, arXiv:1512.09129 [hep-ph]; A. Dasgupta, M. Mitra and D. Borah, arXiv:1512.09202 [hep-ph].

[22] L. J. Hall, K. Harigaya and Y. Nomura, arXiv:1512.07904 [hep-ph];

[23] K. M. Patel and P. Sharma, arXiv:1512.07468 [hep-ph].

[24] R. Ding, L. Huang, T. Li and B. Zhu, arXiv:1512.06560 [hep-ph].

[25] B. C. Allanach, P. S. B. Dev, S. A. Renner and K. Sakurai, arXiv:1512.07645 [hep-ph].

[26] L. Lavoura and J. P. Silva, Phys. Rev. D **47**, 2046 (1993).

[27] K. A. Olive *et al.* [Particle Data Group Collaboration], Chin. Phys. C **38**, 090001 (2014).

[28] T. Moroi and Y. Okada, Mod. Phys. Lett. A **7**, 187 (1992); Phys. Lett. B **295**, 73 (1992); K. S. Babu, I. Gogoladze and C. Kolda, hep-ph/0410085; K. S. Babu, I. Gogoladze, M. U. Rehman and Q. Shafi, Phys. Rev. D **78**, 055017 (2008) [arXiv:0807.3055 [hep-ph]]. S.P. Martin, Phys. Rev. D **81**, 035004 (2010) [0910.2732 [hep-ph]]; P.W. Graham, A. Ismail, S. Rajendran and P. Saraswat, Phys. Rev. D **81**, 055016 (2010) [0910.3020 [hep-ph]].

[29] A. Brignole, G. Degrassi, P. Slavich and F. Zwirner, Nucl. Phys. B **643**, 79 (2002); A. Dedes, G. Degrassi and P. Slavich, Nucl. Phys. B **672**, 144 (2003).

[30] Y. Okada, M. Yamaguchi and T. Yanagida, Prog. Theor. Phys. **85**, 1 (1991); Phys. Lett. B **262**, 54 (1991); A. Yamada, Phys. Lett. B **263**, 233 (1991); J.R. Ellis, G. Ridolfi and F. Zwirner, Phys. Lett. B **257**, 83 (1991); Phys. Lett. B **262**, 477 (1991); H.E. Haber and R. Hempfling, Phys. Rev. Lett. **66**, 1815 (1991).

[31] M. Carena, J. R. Espinosa, M. Quiros and C. E. M. Wagner, Phys. Lett. B **355**, 209 (1995); M. Carena, M. Quiros and C. E. M. Wagner, Nucl. Phys. B **461**, 407 (1996); H. E. Haber, R. Hempfling and A. H. Hoang, Z. Phys. C **75**, 539 (1997); S. Heinemeyer, W. Hollik, and G. Weiglein, Phys. Rev. D **58**, 091701 (1998); M. Carena, H. E. Haber, S. Heinemeyer, W. Hollik, C. E. M. Wagner, and G. Weiglein, Nucl. Phys. B **580**, 29 (2000); S. P. Martin, Phys. Rev. D **67**, 095012 (2003).

[32] https://atlas.web.cern.ch/Atlas/GROUPS/PHYSICS/CombinedSummaryPlots/EXOTICS/index.html#ATLAS_Exotics_Summary.

[33] J. Hisano, hep-ph/0004266.

[34] S. Aoki *et al.* [JLQCD Collaboration], Phys. Rev. D **62**, 014506 (2000) [hep-lat/9911026].

[35] E.Kearns, (2015) http://atlas.web.cern.ch/Atlas/GROUPS/PHYSICS/HIGGS/higgs-xsec/cross.pdf.

[36] Y. Aoki, E. Shintani and A. Soni, Phys. Rev. D **89**, no. 1, 014505 (2014) [arXiv:1304.7424 [hep-lat]].

[37] K. Abe *et al.*, arXiv:1109.3262 [hep-ex].

[38] J. R. Ellis, D. V. Nanopoulos and J. Walker, Phys. Lett. B **550**, 99 (2002) [hep-ph/0205336].

[39] A. D. Martin, W. J. Stirling, R. S. Thorne and G. Watt, Eur. Phys. J. C **63**, 189 (2009) [arXiv:0901.0002 [hep-ph]].

[40] http://atlas.web.cern.ch/Atlas/GROUPS/PHYSICS/HIGGS/higgs-xsec/cross.pdf.

[41] V. Khachatryan *et al.* [CMS Collaboration], arXiv:1410.8812 [hep-ex].

[42] V. Khachatryan *et al.* [CMS Collaboration], arXiv:1512.01224 [hep-ex].

[43] [ATLAS Collaboration], arXiv:1512.01530 [hep-ex].

[44] V. Khachatryan *et al.* [CMS Collaboration], Eur. Phys. J. C **75** (2015) 5, 235 [arXiv:1408.3583 [hep-ex]].

[45] [ATLAS Collaboration], ATLAS-CONF-2012-147.

[46] J. Alwall, M. Herquet, F. Maltoni, O. Mattelaer and T. Stelzer, JHEP **1106**, 128 (2011) [arXiv:1106.0522 [hep-ph]].

[47] J. R. Ellis, J. F. Gunion, H. E. Haber, L. Roszkowski and F. Zwirner, Phys. Rev. D **39**, 844 (1989). M. Drees, Int. J. Mod. Phys. A **4**, 3635 (1989). L. Durand and J. L. Lopez, Phys. Lett. B **217**, 463 (1989).

[48] V. Khachatryan *et al.* [CMS Collaboration], Phys. Rev. D **91** (2015) 9, 092005.

[49] L. E. Ibanez and G. G. Ross, Nucl. Phys. B **368**, 3 (1992).

[50] See for instance, E. J. Chun, S. K. Kang, C. W. Kim and U. W. Lee, Nucl. Phys. B **544**, 89 (1999)